Organ-wide and ploidy-dependent regulation both contribute to cell-size determination: evidence from a computational model of tomato fruit

Valentina Baldazzi, Pierre Valsesia, Michel Génard, Nadia Bertin

Journal of Experimental Botany, Vol. 70, No. 21 pp. 6215–6228, 2019
doi:10.1093/jxb/erz398 Advance Access Publication August 31, 2019
This paper is available online free of all access charges (see https://academic.oup.com/jxb/pages/openaccess for further details)

RESEARCH PAPER

Organ-wide and ploidy-dependent regulation both contribute to cell-size determination: evidence from a computational model of tomato fruit

Valentina Baldazzi[1,2,3,*], Pierre Valsesia[1], Michel Génard[1] and Nadia Bertin[1]

[1] INRA, PSH, 228 route de l'Aerodrome, 84914 Avignon, France
[2] Université Côte d'Azur, INRA, CNRS, ISA, 400 route des Chappes, 06903 Sophia-Antipolis, France
[3] Université Côte d'Azur, Inria, INRA, CNRS, Sorbonne Université, BIOCORE, 2004 route des Lucioles, 06902 Sophia-Antipolis, France

* Correspondence: valentina.baldazzi@inra.fr

Received 15 January 2019; Editorial decision 30 July 2019; Accepted 1 August 2019

Editor: Christine Raines, University of Essex, UK

Abstract

The development of a new organ is the result of coordinated events of cell division and expansion, in strong interaction with each other. This study presents a dynamic model of tomato fruit development that includes cell division, endoreduplication, and expansion processes. The model is used to investigate the potential interactions among these developmental processes within the context of the neo-cellular theory. In particular, different control schemes (either cell-autonomous or organ-controlled) are tested and compared to experimental data from two contrasting genotypes. The model shows that a pure cell-autonomous control fails to reproduce the observed cell-size distribution, and that an organ-wide control is required in order to get realistic cell-size variations. The model also supports the role of endoreduplication as an important determinant of the final cell size and suggests that a direct effect of endoreduplication on cell expansion is needed in order to obtain a significant correlation between size and ploidy, as observed in real data.

Keywords: Cell division, computational model, expansion, endoreduplication, development, tomato fruit.

Introduction

Understanding the mechanisms that underpin fruit development from its early stages is of primary importance for biology and agronomy. In particular, the early stages are highly sensitive to biotic and abiotic stresses, with important consequences on fruit set and yield. The development of a new organ is the result of coordinated events of cell division and expansion. Fruit growth starts immediately after pollination with intensive cell division. As development proceeds, the proliferative activity of cells progressively slows down, giving way to a phase of pure cell enlargement during fruit growth and ripening. In many species, including tomato, the transition from cell division to expansion phases is accompanied by repeated DNA duplications without mitosis, a process called endoreduplication. The exact role of endoreduplication is still unclear. A significant correlation between cell ploidy (i.e. number of DNA copies) and cell size has been observed in different species, including tomato fruit, suggesting a possible role of endoreduplication in the control of organ growth Cheniclet *et al.*, 2005; Breuer *et al.*, 2010; Chevalier *et al.*, 2011). However, several studies have shown that under specific conditions the two processes can be uncoupled to some extent, so that ploidy is not the only determinant of cell size (Bertin, 2005; Cookson *et al.*, 2006).

Understanding the way that the cell division, endoreduplication, and expansion processes interact is crucial for predicting the emergence of important morphological traits (fruit size, mass, shape, and texture) and their dependence on environmental and genetic factors. Historically, there has been a debate between two contrasting views, the cellular versus the organismal theory, that set the control of organ growth at the level of the individual cell or the whole tissue, respectively (reviewed in Beemster *et al.*, 2003; Fleming, 2006; John and Qi, 2008). In recent years, a consensus view has emerged, namely the neo-cellular theory, which considers that although cells are the units of plant morphology, their behavior (division, expansion) is not autonomous, but is coordinated at the organ level by cell-to-cell communication mechanisms (Beemster *et al.*, 2003; Tsukaya, 2003; Sablowski and Carnier Dornelas, 2014). The existence of non-autonomous cell control of organ development has been demonstrated in Arabidopsis leaves (Kawade *et al.*, 2010) but the underlying modes of action remain unclear and are often species- or organ-specific (Ferjani *et al.*, 2007; Horiguchi and Tsukaya, 2011; Norman *et al.*, 2011; Han *et al.*, 2014; Okello *et al.*, 2015).

Computational models offer a unique tool to express and test biological hypotheses in a well-defined and controlled manner, and perhaps not surprisingly they have been used extensively to investigate the relationships between organ development and the underlying cellular processes. Many studies have addressed the question of organogenesis, relating local morphogenetic rules and cell mechanical properties with the emerging patterns near the meristem (Dupuy *et al.*, 2010; Robinson *et al.*, 2011; Kuchen *et al.*, 2012; Lucas *et al.*, 2013; Boudon *et al.*, 2015; Löfke *et al.*, 2015; von Wangenheim *et al.*, 2016). At the tissue scale, a few models have addressed the issue of cell size variance based on observed kinematic patterns of cell division or growth rates, with particular attention being paid to the intrinsic stochasticity of processes related to the cell cycle (Roeder *et al.*, 2010; Asl *et al.*, 2011; Kawade and Tsukaya, 2017). In most of these models, cell expansion is simply described via an average growth rate, possibly modulated by the ploidy level of the cell, without any reference to the underlying molecular mechanisms or to the environmental conditions.

To our knowledge, very few attempts have been made to explicitly model the interactions among cell division, expansion, and endoreduplication at the scale of organ development. Fanwoua *et al.* (2013) proposed a model of tomato fruit development that integrates cell division, expansion, and endoreduplication processes based on a set of biologically inspired rules. The fruit is described by a set of q classes of cells with the same age, ploidy, and mass. Within each class, cell division and endoreduplication are described as discrete events that take place within a well-defined window of time whenever a specific mass-to-ploidy threshold is reached. Cell growth in dry mass is modeled following a source–sink approach as a function of thermal time, cell ploidy, and external resources. The model is able to qualitatively capture the effect of environmental conditions (temperature, fruit load) on the final fruit dry mass, but hypotheses and parameters are hard to validate as comparisons to experimental data are lacking. Moreover, the water content of the cell is not considered, preventing the analysis of cell volumes.

Baldazzi *et al.* (2012, 2013) have developed an integrated model of tomato fruit development that explicitly accounts for the dynamics of cell proliferation as well as for the mechanisms of cell expansion, in both dry and fresh mass, based on biophysical and thermodynamical principles. In this present study, a new version of this model is proposed that includes cell endoreduplication. The model is used to investigate different hypotheses concerning the regulation and the interaction among cellular processes, with special attention being paid to the importance of an organ-wide regulation on cell growth and on the potential effect of endoreduplication on cell expansion. We focus on wild-type organ development and we examine the effects of organ-wide or cell ploidy-dependent regulation on the dynamics of cell expansion. To this end, different control schemes (either cell-autonomous or organ-controlled, with or without a ploidy effect on cell expansion) are tested *in silico* by means of specific model variants. Simulation results are analysed and compared to cell-size distributions observed in the fruit pericarp of two contrasting genotypes, a cherry tomato and a large-fruited variety.

The model shows that a pure cell-autonomous control cannot reproduce the experimental cell-size distribution, and organ-wide and ploidy-dependent controls are required in order to obtain realistic cell sizes. In particular, a direct effect of endoreduplication on cell expansion is needed in order to obtain a significant correlation between size and ploidy, as observed in real data.

Materials and methods

Experimental data

Two datasets were collected from two glasshouse experiments performed at INRA Avignon (southern France) in 2004 and 2007 on large-fruited (cv Levovil) and cherry (cv. Cervil) tomato genotypes of *Solanum lycospersicum* L.

In the 2004 experiment fruit were collected from April to May (planting in February) whereas in 2007 the fruit were sampled from October to December (planting in August). Plants were grown according to standard cultural practices. Trusses were pruned in order to homogenize truss size along the stem within each genotype. The maximum number of flowers left on each inflorescence was 12 for Cervil and six for Levovil. Flowers were pollinated by bumblebees. Air temperature and humidity were recorded hourly in each experiment and input in the model as external signals.

In both experiments, flower buds and fruit were sampled at different time-points relative to the time of flower anthesis (full-flower opening). Fruit fresh and dry mass and pericarp fresh mass were systematically measured at all time-points. Pericarp dry mass was estimated by assuming a dry mass content equivalent to that of the whole fruit.

In 2004, half of the fruit pericarps were then analysed by flow cytometry and the other half were used for the determination of cell number. The number of pericarp cells was measured after tissue dissociation according to a method adapted from that of Bünger-Kibler and Bangerth (1982) and detailed in Bertin *et al.* (2003). Cells were counted in aliquots of a cell suspension under an optical microscope using Fuchs–Rosenthal chambers and Bürker chambers for the large and small fruit, respectively. Six to eight aliquots per fruit were observed and the cell number for the whole pericarp was calculated according to the dilution and observation volumes. Ploidy was measured in the pericarp tissue as described in Bertin *et al.* (2007). The mean value of up to three measurements per fruit (sometimes restricted by the fruit size) was included in the analysis.

In the 2007 experiment, the dynamics of cell number (but not endoreduplication) were measured following the same method as in the 2004 experiment. In addition, cell-size distributions (smallest and largest

radii and 2D-surface) in the cell suspension aliquots were measured using the ImageJ software (https://imagej.nih.gov/ij/). Samples of ~20–25 cells per fruit pericarp were measured randomly for several different fruit. Cell-size distributions were measured on ripe fruit at ~43 d after anthesis (DAA) for Cervil and 60 DAA for Levovil.

Model description

The model is composed of two interacting modules, both originating from previously published models (Fishman and Génard, 1998; Bertin *et al.*, 2007; Liu *et al.*, 2007). The fruit is described as a collection of cell populations, each one having a specific age, ploidy, and volume, which evolve and grow over time during fruit development. Two cell classes are defined: the proliferating cells and the expanding-endoreduplicating cells (Fig. 1). The division–endoreduplication module governs the evolution of the number of cells in each of the classes, their age (initiation date), and ploidy level based on genotype-specific parameters (Bertin *et al.*, 2007). At each mitotic cycle, a fraction of proliferating cells proceeds through division whilst the remaining ones enter the expansion phase: a new group of expanding cells is created, together with an array of sub-classes of possible ploidy levels p. At initialization of the group, all expanding cells are put into the 4C level.

It is assumed that the onset of endoreduplication coincides with the beginning of the expansion phase. As the endocycles proceed, in each group of expanding cells a fraction σ of the cells increases its ploidy level p by a factor 2 and the distribution of cells across the different ploidy levels is updated.

At any time, the mass (both fresh and dry components) of expanding cells is computed by a biophysical expansion module according to characteristics of the cell (age, ploidy) and depending on available resources and environmental conditions (Fishman and Génard, 1998; Liu *et al.*, 2007). Briefly, cell expansion is described by iteratively solving the Lockhart equation that relates the rate of volume increase to the internal pressure and mechanical properties of the cell (Lockhart, 1965). Flows of water and solutes across the membrane are described by thermodynamic equations and depend on environmental conditions. The relative importance of each transport process may vary according to the fruit developmental stage, depending on specific developmental control. A full description of the model equations can be found in Supplementary Protocol S2 at *JXB* online.

The model assumes that all cells have equal access to external resources, independently from the number of cells (i.e. no competition). All the parameters of the division-endoreduplication module are considered to be independent from environmental conditions for the time being.

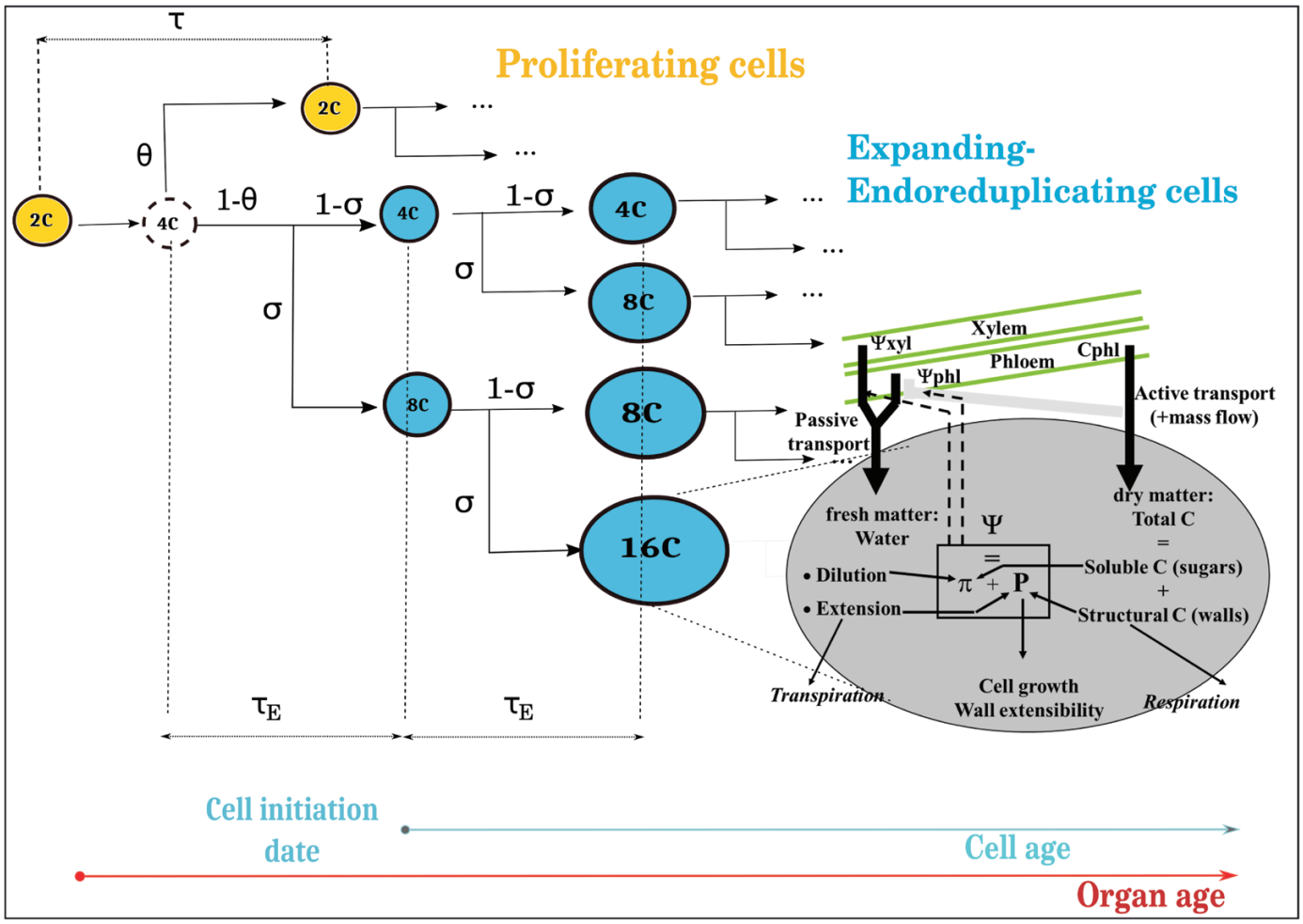

Fig. 1. Scheme of the integrated model. The fruit is described as a collection of cell populations, each one having a specific age, ploidy, and volume. Cells can be either proliferating or expanding-endoreduplicating. The number of cells in each class is predicted by the division-endoreduplication module, assuming a progressive decline of the proliferating activity of the cells. Expanding cells grow according to the expansion module, which provides a biophysical description of the main processes involved in carbon and water accumulation. It is assumed that the onset of endoreduplication coincides with the beginning of the expansion phase. Two timescales are recognizable in the model: the organ age, i.e. the time since the beginning of the simulation; and the cell age, i.e. the time since the cell left the mitotic cycle and entered the expansion-endoreduplication phase. Depending on the model variant, cell expansion may be modulated by organ age (organ-wide control) and/or by cell ploidy. (This figure is available in colour at *JXB* online.)

Model initialization and input

The model starts at the end of the pure division phase, when the proliferative activity of the cells declines and the expansion phase begins (Baldazzi *et al.*, 2013). For the Cervil (cherry) genotype this corresponds to ~8 d before anthesis and to 3 d before anthesis for the Levovil (large-fruited) genotype (Bertin *et al.*, 2007). The initial number of cells for the 2007 experiment, n_0, was estimated as 3.3×10^3 for Cervil and as 4.6×10^4 for Levovil, based on a few measurements. At the beginning of the simulation, all cells are presumed to be proliferating with a ploidy level of 2C (a transient ploidy of 4C during the cell cycle is not considered here). Proliferating cells are presumed to have a constant cell mass equal to the initial value, m_0, as often observed in meristematic cells (homogeneity in cell size) (Sablowski and Carnier Dornelas, 2014; Serrano-Mislata *et al.*, 2015).

The initial mass of the fruit is therefore $M_{fruit}(0) = n_0 m_0 = n_0(w_0+s_0)$, where w_0 and s_0 are initial cell water and dry mass, respectively. At any time, cells leaving the proliferative phase start to grow, from an initial mass $2m_0$ and a ploidy level of *4C*, according to the expansion model.

Cell expansion depends on environmental conditions and on resources provided by the mother plant. The phloem sugar concentration is assumed to vary daily between 0.15 M and 0.35 M whilst the stem water potential oscillates between –0.05 MPa and –0.6 MPa, i.e. typical pre-dawn and minimal stem water potentials as measured for the two genotypes. Temperature and humidity are provided directly by real-time recording of greenhouse climatic conditions.

Choice of the model variants: control of cell expansion capabilities

In the integrated model, a number of time-dependent functions account for the developmental regulation of cell metabolism and physical properties during the expansion phase (Liu *et al.*, 2007; Baldazzi *et al.* 2013). Two characteristic time-scales are recognizable in the model: the *cell age*, i.e. the time spent since an individual cell has left the proliferative phase; and *organ age*, i.e. the time spent since the beginning of the simulation (Fig. 1). Depending on the settings of the corresponding time-dependent functions, different cellular processes may be put under cell-autonomous or non- autonomous control (hereafter termed as organ-wide control), allowing for an *in silico* exploration of alternative control hypotheses in the context of the cellular and organismal theories. Moreover, a direct effect of cell DNA content on cell expansion capabilities may be tested according to biological evidence (Sugimoto-Shirasu and Roberts, 2003; Chevalier *et al.*, 2011; Edgar *et al.*, 2014).

As a default, all cellular processes are presumed to depend on cell age (cell-autonomous control) with the only exception of cell transpiration, which is computed at the organ scale on the basis of fruit external surface and skin conductance, and then distributed back to individual cells proportionally to their relative water content (see Supplementary Protocol S2 for a full description of the integrated model).

Based on literature information and on preliminary tests (Baldazzi *et al.*, 2013, 2017), the switch between symplastic and apoplastic transport, λ_p, has been selected as the candidate process for an organ-wide control. Indeed, intercellular movement of macromolecules across plasmodesmata has been shown to be restricted by organ age in tobacco leaves (Crawford and Zambryski, 2001; Zambryski, 2004) and it is known to be important for cell-to-cell communication (Han *et al.*, 2014).

The exact mechanisms by which cell DNA content may affect cell expansion currently remain unknown. Based on literature information and common sense, three distinct mechanisms of action of endoreduplication on cell expansion were hypothesized and tested by means of the model (Fig. 2).

(1) Endoreduplication has been often associated with elevated protein synthesis and transcriptional activity (Chevalier *et al.*, 2014), suggesting a general activation of the nuclear and metabolic machinery of the cell to sustain cell growth (Sugimoto-Shirasu and Roberts, 2003). Given these facts, a first hypothesis assumes an effect of endoreduplication on cell expansion as a ploidy-dependent maximal import rate for carbon uptake (ν_m). For the sake of simplicity, and in the absence of any information, the relationship was presumed to be linear across the number of endocycles. The corresponding equation, as a function of the cell DNA content (DNA_c; 2 for dividing cells, 4 to 512 for endoreduplicating cells), was as follows:

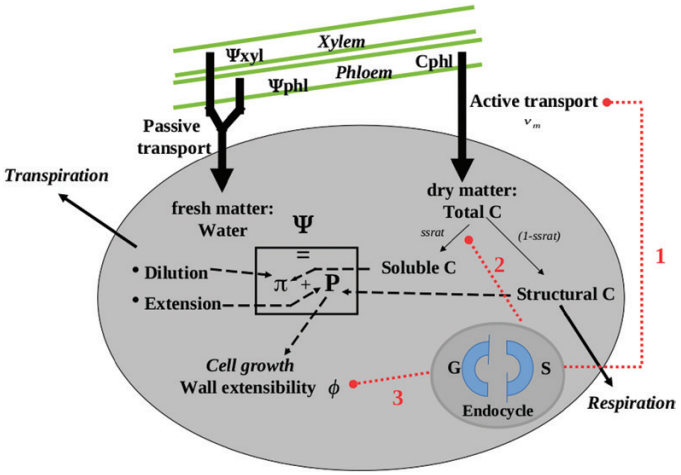

Fig. 2. Schematic representation of the three hypothetical mechanisms of interaction between cell ploidy and cell expansion. (1) Cell ploidy may affect the carbon uptake rate. (2) Ploidy may increase the fraction of soluble components in the cell, thus increasing the osmotic potential. (3) Ploidy may affect cell wall extensibility. (This figure is available in colour at *JXB* online.)

$$\nu_m = \nu^0 \log_2 (DNA_c)$$

where ν^0 is the mean carbon uptake activity per unit mass.

(2) Assuming that cell shape remains the same with increasing ploidy, endoreduplicating cells are characterized by a reduced surface-to-volume ratio with respect to 2C cells (Schoenfelder and Fox, 2015). As a consequence, it is tempting to suppose that one possible advantage of a high ploidy level may reside in a reduction of carbon demand for cell wall and structural units (Barow, 2006; Pirrello *et al.*, 2018). We speculated that such an economy may affect cell expansion capabilities in two ways. First, the metabolic machinery could be redirected towards the synthesis of soluble components, thus contributing to the increase of cell internal pressure and consequent volume expansion.

In the original expansion model, the *ssrat* fraction of soluble compound within the cell is developmentally regulated by the age, *t*, of the cell (Baldazzi *et al.* 2013): at early stages a large fraction of carbon is devoted to the synthesis of structural components (proteins, lipids, and wall components), reducing the quantity of carbon available for osmotic regulation (Carrari *et al.*, 2006, Colombié *et al.*, 2014). Accordingly, the *ssrat* fraction is an increasing function of time, up to a maximal value (b_{ssrat}).

$$ssrat = b_{ssrat}\left(1 - e^{-a_{ssrat}t}\right) + ssrat_0$$

In the presence of a ploidy effect, the final b_{ssrat} value was further increased as:

$$b_{ssrat} = b^0{}_{ssrat} \log_2 (DNA_c)$$

(3) Second, 'exceeding' carbon may be used to increase the rate of cell wall synthesis or that of related proteins, possibly resulting in an increase of cell wall extensibility as it has been shown in other systems (Proseus and Boyer, 2006, Jégu *et al.*, 2013).

In the original expansion model of tomato (Liu *et al.*, 2007), cell wall extensibility, ϕ, declines during cell maturation (Proseus *et al.*, 1999) as the result of changes in the expression of cell wall-related enzymes (Thompson *et al.*, 1998; Cosgrove, 2016):

$$\phi = \phi_{min} + \frac{(\phi_{max} - \phi_{min})}{1 + e^{k(t-t_0)}}$$

where ϕ_{min} and ϕ_{max} are the minimal and the maximal cell wall extensibility, respectively, and *k* is the time-constant of ϕ relaxation above time t_0.

In the presence of a ploidy effect, the maximal cell wall extensibility was increased as:

$$\phi_{max} = \phi^0{}_{max} \log_2 (DNA_c)$$

The individual and combined effects of organ-wide and ploidy-dependent control of cell expansion were investigated and compared to a full cell-autonomous model. A total of 10 model variants were tested for each genotype, following the experimental design shown in Table 1.

Model calibration

Calibration was performed using a genetic algorithm in the R software (library 'genalg'; https://CRAN.R-project.org/package=genalg). Due to data limitations, a three-step procedure was used for each tomato genotype.

First, the division-endoreduplication module (seven parameters) was calibrated with data from the 2004 experiment by comparing measured and simulated values of the total pericarp cell number and the proportion of cells in different ploidy classes throughout fruit development. In particular, this allowed the estimation of the mean duration of the endocycle (τ_E) and the proportion (σ) of the cells performing a new endoreduplication round within every period τ_E.

The best-fitting values of σ and τ_E were selected and kept fixed for the second phase of the calibration, assuming that they have little dependence on environmental conditions (Bertin, 2005). The dynamics of cell division (five parameters) were then re-estimated using cell numbers measured in the 2007 experiment, in order to account for environmental regulation of the mitotic cell cycle (see Supplementary Protocol S3). The best-fitting parameters were selected and used for the third and final calibration step.

The expansion module was calibrated using the evolution of pericarp fresh and dry mass from the 2007 experiment, for which cell size distributions were available. However, it should be noted that data for measured cell sizes were *not* used for the fitting process.

Six parameters were selected for calibration based on a previous sensitivity analysis (Constantinescu *et al.*, 2016), whilst the others were fixed to the original values (Fishman and Génard, 1998; Liu *et al.*, 2007; Baldazzi *et al.*, 2013). An additional parameter was estimated for model variants M3–M24 (Table 1) in order to correctly evaluate the strength of the ploidy-dependent control (see Supplementary Protocol S3 for more information).

Due to their different structures, the expansion module was calibrated independently for each model variant. The quality of model adjustment was evaluated using a normalized root mean-square error (NRMSE):

$$NRMSE(x) = 100 \frac{\sqrt{\frac{1}{n}\sum [O_i - S_i(x)]^2}}{\frac{1}{n}\sum O_i}$$

where O_i and S_i are, respectively, the observed and simulated values of pericarp fresh or dry mass, and n is the number of observations.

Table 1. *Experimental design showing the characteristics of the 10 model variants tested in the study*

Model variant	Organ control	Endoreduplication effect		
	Symplastic transport	Active C uptake	C allocation	Wall plasticity
M0				
M1	✓			
M2	✓	✓		
M3	✓		✓	
M4	✓			✓
M5		✓		
M6			✓	
M7				✓
M23	✓	✓	✓	
M24	✓	✓		✓

$x = \{x_1, x_2 \ldots x_p\}$ is the parameter set of the evaluated solution. The smaller the NRMSE the better the goodness-of-fit. Generally, NRMSE<20% is considered good, 20%<NRMSE<30% is considered fair, and values over 30% are considered poor.

Between three and five estimations were performed for each model variant and genotype.

Solution selection and model comparisons

For each calibration solution, the corresponding cell-size distribution at fruit maturity (i.e. 43 DAA for Cervil, 60 DAA for Levovil) was predicted by the model and compared to the measured data.

A semi-quantitative comparison approach was used due to the limited experimental information available: the general distribution characteristics (shape, positioning, and dispersion) were characterized rather than having a 'perfect fit'. To this end, eight descriptive statistical indicators, $m(i)$, were computed for each solution and compared to those derived from real-data distribution, namely: skewness and kurtosis (shape of distribution); mean and median cell size (positioning); standard deviation (SD) and median absolute deviation (MAD) (data dispersion); and maximal and minimal cell size (data dispersion). Confidence intervals (CI, 95%) for the experimental distribution indicators were estimated using a Bootstrap approach on 10 000 samples.

Based on the scores for these indicators, the distance, D, between the predicted and the observed distribution was quantified as the Euclidean distance between each indicator $m(i)$ and its corresponding measured value, weighted by the amplitude of the confidence interval (DeltaCI) of the indicator itself:

$$D = \sqrt{\frac{\sum_{i=1}^{8} [m_{model}(i) - m_{data}(i)]^2}{DeltaCI(i)}}$$

For each model variant, the selection of the best calibration solution was performed based on a compromise between quality of the fit at the whole-fruit scale (as measured by the total NRMSE) and quality of the corresponding cell-size distribution (as measured by D; see Supplementary Protocol S3). Estimated parameters for the retained solution are given in Tables S3 and S4 of Supplementary Protocol S3.

In order to compare the distributions issued from the different models, a principal component analysis (PCA) was performed on the eight descriptors of cell distribution arising from each model estimation. The 'ade4' library of the R software was used for this purpose (https://CRAN.R-project.org/package=ade4).

Results

A characteristic right-tailed distribution of cell areas

The distribution of cell sizes at a given stage of fruit development directly depends on the particular cell division and expansion patterns followed by the organ up to the time in question. Any change in the cell division or expansion rate will have a consequence on the shape and position of the resulting distribution.

For both the tomato genotypes considered in this study, the distribution of pericarp cell areas at the mature stage showed a typical right-tailed shape (Fig. 3), compatible with a Weibull or a Gamma distribution (Supplementary Protocol S1). The observed cell sizes spanned up to two orders of magnitude, with cell areas (cross-section) ranging from 0.004 mm to 0.08 mm^2 for the cherry Cervil genotype and from 0.005 mm to 0.28 mm^2 for the large-fruited Levovil (Tables 2, 3). The mean cell area was calculated to be 0.026 mm^2 for the cherry genotype and 0.074 mm^2 for the large-fruited genotype, and these values are in agreement with data from other tomato

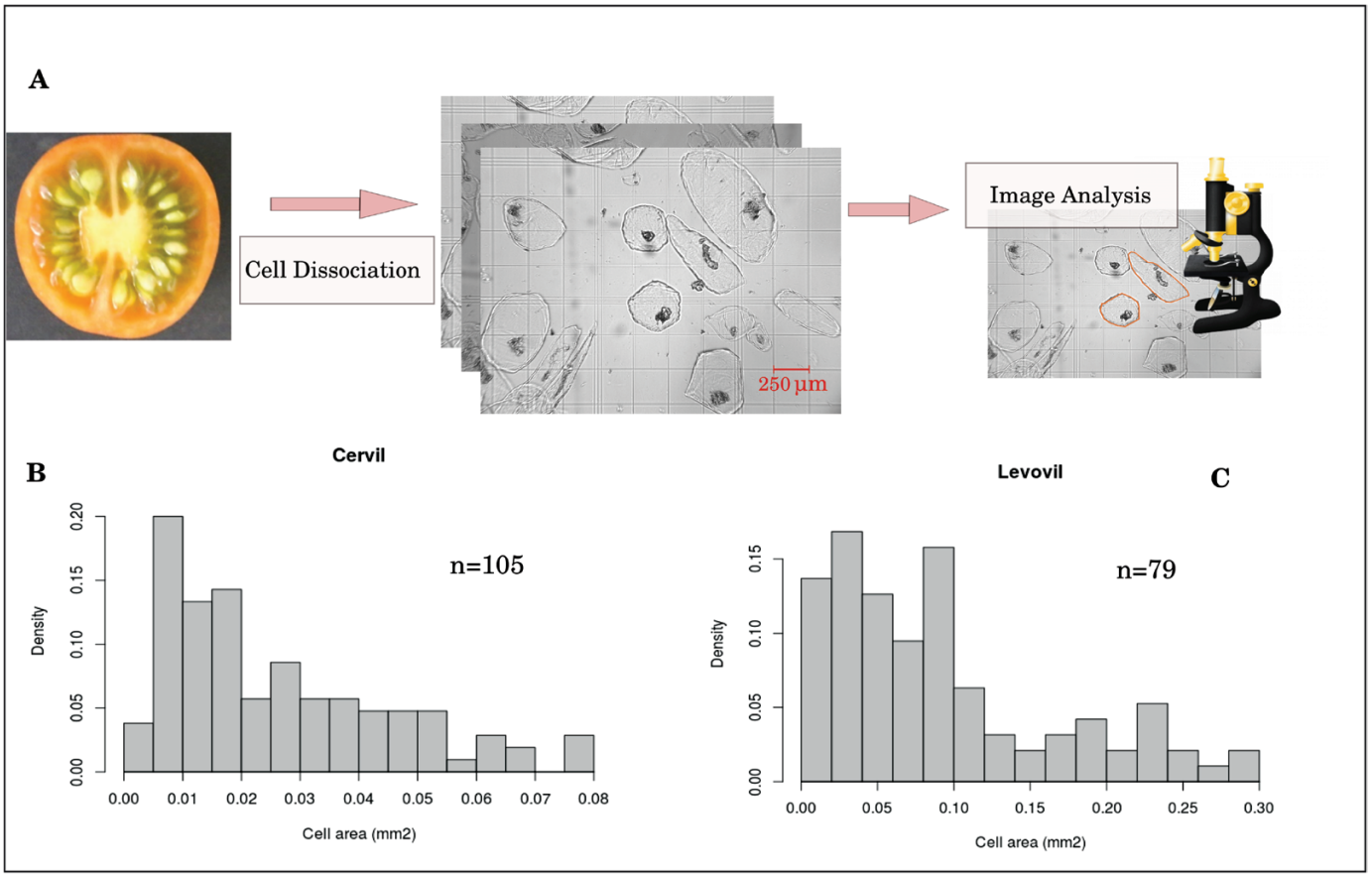

Fig. 3. (A) Schematic representation of the experimental procedure for estimation of cell size. About half of the fruit pericarp was subjected to tissue dissociation. Cells were divided into different aliquots and spotted onto clean glass slides before examination under a microscope. Images were captured with a digital camera and analysed using the ImageJ software. (B, C) Measured cell-size distributions at fruit maturity, for (B) the Cervil cherry tomato genotype, and (C) the Levovil large-fruited genotype. (This figure is available in colour at *JXB* online.)

varieties (Bertin, 2005; Renaudin *et al.*, 2017). Data dispersion was higher for the large-fruited genotype, but the shape of the distribution, as measured by its skewness and kurtosis values, was pretty similar for both varieties.

In the following sections, the effects of specific control mechanisms on the predicted cell area distribution are analysed in detail, based on the results obtained for the selected calibration solution (see 'Solution selection' in the Methods). The corresponding

Table 2. *Statistical descriptors for the measured and predicted cell area distributions for the cherry tomato Cervil genotype*

Model	Fruit mass		Cell distribution							
	Fit quality		Shape		Positioning				Dispersion	
	NRMSE FM	NRMSE DM	Skewness	Kurtosis	Mean	Median	Min.	Max.	SD	MAD
Experimental data (CI 95%)			0.97 (0.63–1.34)	3.13 (2.3–4.4)	0.026 (0.023–0.030)	0.019 (0.016-0.025)	0.0039 (–)	0.08 (> 0.069–0.08)	0.019 (0.017–0.022)	0.016 (0.013–0.023)
M0	29.46	25.06	0.05	1.9	0.025	0.025	0.024	0.026	0.0003	0.0003
M1	28.53	24.40	1.21	4.2	0.025	0.024	0.023	0.027	0.0008	0.0005
M2	29.44	25.65	1.66	11.4	0.023	0.023	0.016	0.13	0.005	0.004
M3	22.45	22.36	3.5	18	0.022	0.020	0.017	0.059	0.006	0.002
M4	24.86	24.29	0.59	3.8	0.022	0.022	0.019	0.031	0.0015	0.0014
M5	31.13	26.36	1.48	9.2	0.024	0.022	0.017	0.11	0.004	0.004
M6	25.57	24.66	−0.46	5.4	0.023	0.023	0.017	0.027	0.0006	0.0006
M7	27.0	25.07	0.42	3.16	0.023	0.023	0.019	0.038	0.0019	0.0019
M23	22.93	22.50	2.48	13.8	0.022	0.021	0.012	0.12	0.007	0.004
M24	25.72	24.90	1.44	7.3	0.022	0.022	0.012	0.14	0.006	0.005

NRMSE, normalized root mean-square; FM of pericarp, fresh mass; DM, dry mass of pericarp; MAD, median absolute deviation; CI, confidence interval. Dark shading indicates satisfactory agreement with the experimental data (i.e. NRMSE<25 and moment values within the CI of the experimental measurements) and light shading indicates partial agreement (NRMSE between 25–30, moment values near the limit of the CI).

Table 3. *Statistical descriptors for the measured and predicted cell area distribution for the large-fruited tomato Levovil genotype*

Model	Fruit mass		Cell distribution							
	Fit quality		Shape		Positioning				Dispersion	
	NRMSE FM	NRMSE DM	Skewness	Kurtosis	Mean	Median	Min	Max	Sd	MAD
Experimental data (CI 95%) (red only)			0.97 (0.60–1.42)	3.15 (2.25–4.8)	0.094 (0.079–0.11)	0.082 (0.059–0.092)	0.008 (–)	0.29 (0.23–0.29)	0.072 (0.061–0.085)	0.058 (0.041–0.092)
M0	30.04	34.38	–2.47	9.14	0.075	0.082	0.00049	0.085	0.016	0.005
M1	25.07	28.59	0.76	3.37	0.065	0.058	0.00049	0.15	0.032	0.022
M2	24.02	30.21	1.02	4.19	0.062	0.055	0.00049	0.31	0.040	0.021
M3	23.65	24.75	1.8	7.05	0.059	0.050	0.00049	0.21	0.033	0.018
M4	25.35	29.67	0.78	3.9	0.066	0.062	0.00049	0.19	0.032	0.027
M5	31.06	35.58	2.4	8.58	0.072	0.078	0.00049	0.090	0.016	0.006
M6	30.39	33.64	–2.48	9.14	0.071	0.078	0.00049	0.081	0.016	0.005
M7	31.40	35.80	0.61	3.38	0.068	0.062	0.00049	0.17	0.032	0.026
M23	24.51	27.48	0.99	4.47	0.062	0.056	0.00049	0.22	0.033	0.030
M24	24.83	30.93	6.65	77.54	0.056	0.038	0.00049	1.1	0.064	0.022

NRMSE, normalized root mean-square; FM of pericarp, fresh mass; DM, dry mass of pericarp; MAD, median absolute deviation; CI, confidence interval. Dark shading indicates satisfactory agreement with the experimental data (i.e. NRMSE<25 and statistical indicators within the CI of the experimental measurements) and light shading indicates partial agreement (NRMSE between 25–30, moment values near the limit of the CI).

statistical descriptors are given in Tables 2 and 3 for the Cervil and Levovil genotypes, respectively. Note that the predicted minimal cell sizes for Levovil were systematically lower than experimental measurements and corresponded to the size of proliferating cells (assumed to be constant in the present version of the model).

A simple cell-autonomous control scheme leads to unrealistic cell-size distribution

As a benchmark model, we first considered the case of a simple cell-autonomous control without a ploidy-dependent effect (variant M0 of the model; Table 1). Accordingly, two cells with the same age, even if initiated at different fruit developmental stages, behave identically in respect to carbon metabolism, transport, and wall mechanical properties. In this scheme, therefore, cell-size variations are derived exclusively from the dynamics of cell division, which cause a shift in the initiation date for different cohorts of cells. When applied to our genotypes, the cell-autonomous model was able to reproduce the observed pericarp mass dynamics but the corresponding cell-size distribution was extremely narrow (Tables 2, 3).

Including an organ-wide mechanism that controls cell size (model M1) introduced a source of variance among cells. In this case, two cells of the same age that were initiated at different fruit stages do *not* behave identically, resulting in different expansion capabilities and growth patterns (Fig. 4; Baldazzi *et al.*, 2013). As a result, standard deviation doubled and skewness increased towards small positive values, indicating a slightly right-tailed cell-size distribution, both for the cherry and large-fruited genotypes (Tables 2, 3). However, the maximum cell size predicted by the model remained much smaller than expected, suggesting that a mechanism controlling cell expansion was lacking in the model.

Endoreduplication and cell growth: possible action and genotypic effects

The suggestion that nuclear ploidy level may be important for control of cell size has often been reported in the literature. However, the molecular mechanism by which ploidy could modulate the expansion capacity of the cell remains elusive. In our study, three cell properties were selected as possible targets of ploidy-dependent modulation: the maximum carbon uptake rate; carbon allocation between soluble and non-soluble compounds; and cell wall plasticity (see Methods). These three hypotheses were tested on both genotypes, in combination or not with an organ-wide control.

A principal component analysis was performed on eight statistical descriptors of cell-size distribution in order to compare the predictions of the different models (see Methods and Tables 2, 3). For both genotypes, the first two principal components explained ~90% of the observed variance (Figs 5, 6). Separation was mainly performed by the first principal component on the basis of the width of the distribution (SD, MAD, and maximal cell size) in one direction, and its mean and median values in the other direction.

As already noted, the model with simple cell-autonomous control was characterized by narrow distributions that were centered around a larger mean (and median) value. The addition of an organ or ploidy effect on cell expansion resulted in an increase in cell-size variance and skewness, shifting the distribution towards the right-tailed shape of the observed data (Tables 2, 3). Models combining an organ-wide and a ploidy-dependent control were closer to the experimental data, although they could not fully match the observed distribution in the case of the cherry tomato genotype.

When analysed in detail, the results showed that the relative importance of the organ-wide and the ploidy-dependent control of cell expansion was genotype-dependent. In the case of Levovil, organ-wide control turned out to be the major regulatory mode. With the exception of M7, all the models without organ-control (M0, M5, M6) completely failed to reproduce the observations, resulting in very narrow and left-tailed cell-size distributions. Organ-wide coordination of cell expansion appeared to be the main factor responsible for positive skewness of cell-size distribution whilst the addition of an endoreduplication-mediated modulation of cell expansion

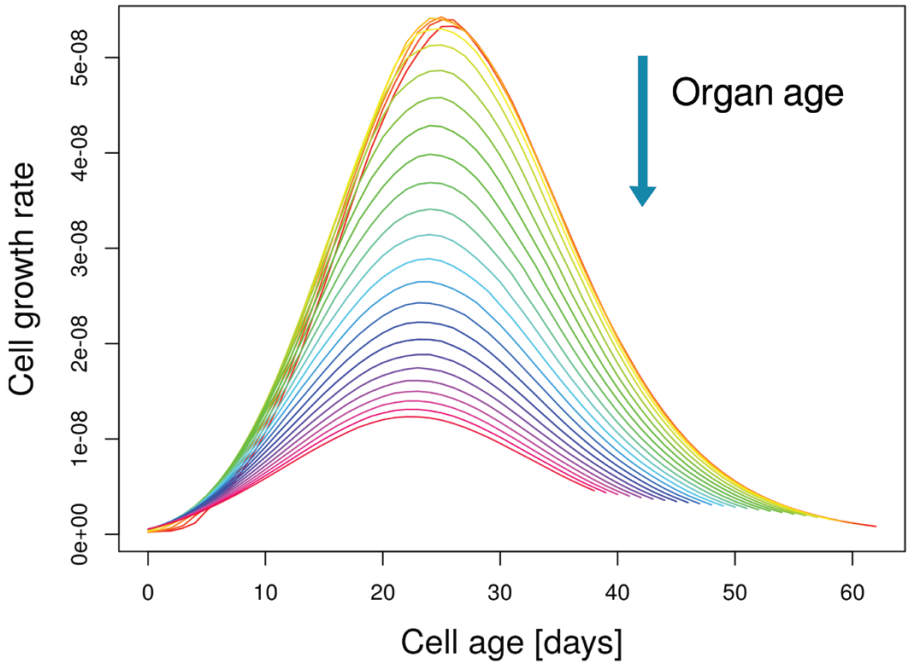

Fig. 4. Effect of an organ-wide control on the cell growth rate. Cells that enter the expansion phase late during organ development (i.e. greater organ age) have a lower growth rate due to the progressive reduction of the symplastic carbon transport. The simulations were obtained with model M1 (Table 1) applied to the large-fruited Levovil genotype. (This figure is available in colour at *JXB* online.)

capabilities on its own resulted only in a marginal improvement of the performance of the models.

The relative roles of ploidy-dependent and organ-wide control of cell growth appeared more balanced in the cherry tomato Cervil. Models including an organ-wide (M1) *or* a ploidy-mediated control of cell expansion (M5–M7) both resulted in very narrow and quite symmetric distributions. The concomitant action of both control mechanisms was needed in order to get the expected right-tailed distribution and realistic cell size variations (models M2–M4, M23, and M24). The two mechanisms thus seemed to act in synergy to increase cell expansion and final cell size.

A direct influence of endoreduplication on cell expansion is needed to produce a correlation between cell size and ploidy

A strong correlation has been often reported between cell size and ploidy level. This may be partly innate to the temporal evolution of endoreduplication, as cells with a high ploidy have necessarily had more time to growth without being halved by cell division. On this basis, some authors have claimed that the observed correlation between size and ploidy is just a matter of time and that there is no need to invoke any direct effect of endoreduplication on cell growth to explain the data (Roeder *et al.*, 2010; Robinson *et al.*, 2018).

We checked this intuitive view with the help of our modelling framework. A linear regression analysis between cell size and DNA content at fruit maturity was performed for all our models and the results are shown in Table S5 in Supplementary Protocol S4).

For both genotypes, no correlations were found for models M0 and M1 (Figs 7, 8) due to the asynchrony in the cell division and endoreduplication patterns. Indeed, cells can attain the same ploidy level following different temporal sequences of expansion and endocycle events, leading to a large variability of possible cell sizes and ages within the same ploidy class. As long as ploidy level and growth rate are independent (as in models M0 and M1), the specific endoreduplication pattern has no consequence on the final cell size: variations in cell sizes simply reflect variations in cell ages and no correlation is found, on average, between the ploidy and size.

A direct effect of ploidy on cell expansion rate was needed in order to get a non-zero correlation between ploidy and size in our model (Figs 7, 8, right panels). In particular, models in which the ploidy level affected the carbon import rate (M2, M5, M23, M24) led to a significant positive correlation between ploidy and size ($P<0.001$) for both genotypes (Table S5, Supplementary Protocol S4). In these models, the observed increase in cell size with increasing ploidy level was directly linked to enhanced cell expansion capabilities, and significant correlations were found between ploidy and maximal cell growth rate (Table S6, Supplementary Protocol S4).

Interestingly, the heterogeneity in cell sizes increased with increasing ploidy (Levene test on size variance, $P<0.001$), which was in agreement with previous observations in another tomato variety (Bourdon *et al.*, 2011). Cell size variations were larger for Levovil than for Cervil due to its extended division phase, which increased the variability in the timing of exit from the mitotic phase (Fig.7, right panel).

Discussion

We have described an integrated cell division–expansion model that explicitly accounts for DNA endoreduplication,

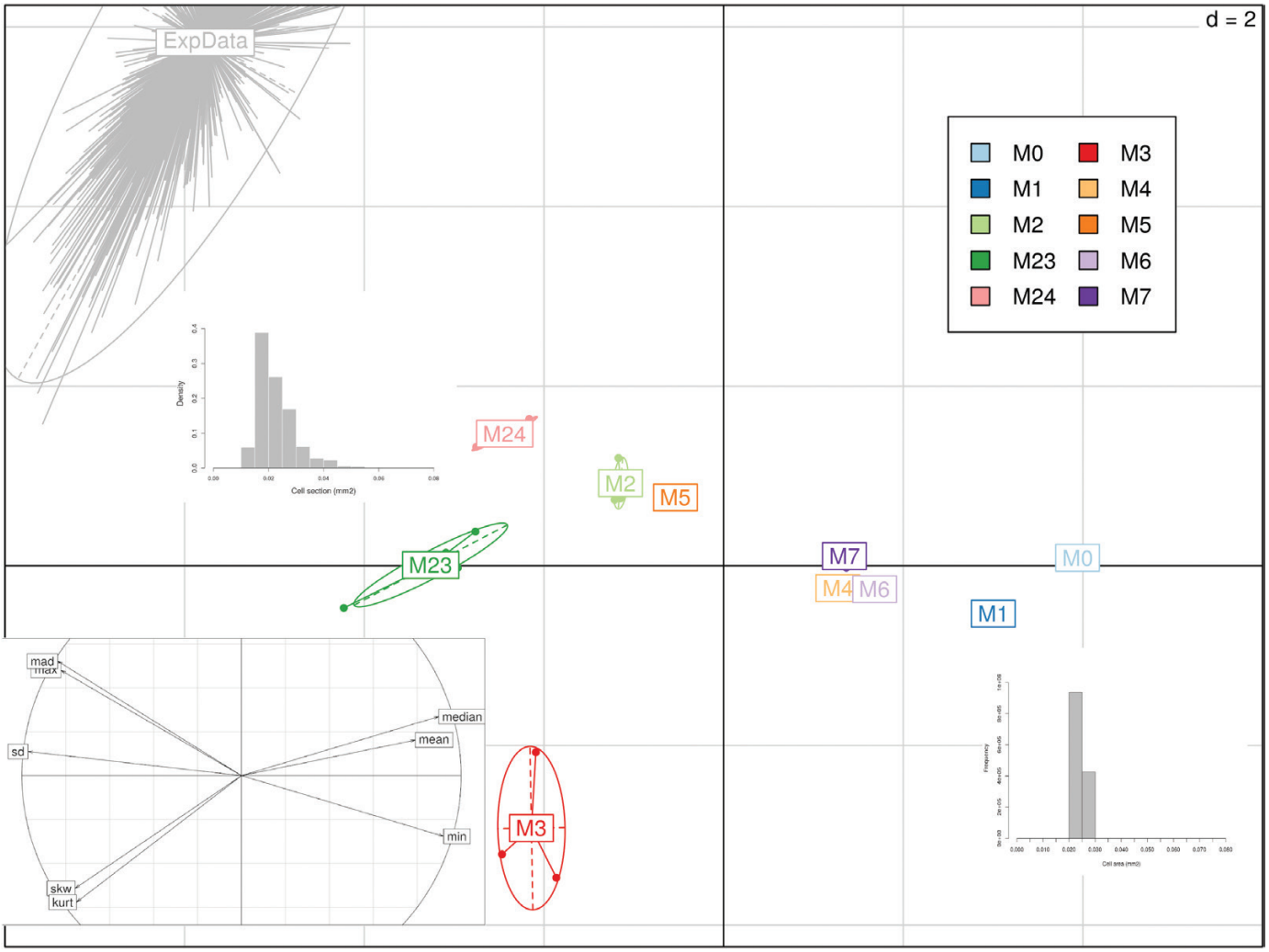

Fig. 5. Principal component analysis (PCA) of cell-size distributions obtained for the cherry tomato genotype Cervil using the model variants M0–M24 (Table 1). The main plot shows the projection of individual distributions on the PC1–PC2 plane (72% and 16% of variance explained, respectively); *d* is the grid unit. Bootstrap results for measured cell size data are also projected (ExpData) as supplementary observations. Typical cell-size distribution shapes are illustrated for the main subgroups. Correlations of the variables with the first two principal components are shown at bottom left.

an important mechanism in tomato fruit development. The model is used to investigate the interactions among cell division, endoreduplication, and expansion processes within the framework of the neo-cellular theory (Beemster *et al.*, 2003).

To this end, 10 model variants with or without a ploidy-dependent and an organ-wide control of cell development (Table 1) were tested and compared to data from two contrasting tomato genotypes. Specific cellular processes were hypothesized as possible targets of both modes of control, based on information from the literature (Fig. 2). It is important to stress that the molecular basis of the presumed forms of regulation are not described in the model and they could involve many molecular players, such as hormones and mechanical signals. Moreover, the existence of other targets for organ-wide or ploidy-dependent regulation cannot be excluded, and neither can the contribution of other mechanisms to the control of cell growth. The objective of the study was thus not to identify the exact mechanism of the interaction between endoreduplication and expansion, but rather to test *if* a direct influence of ploidy on cell expansion, either in combination or not with an organ-wide control, was likely to be involved in the control of fruit growth.

Our model simulations showed that a pure cell-autonomous control was unable to reproduce the observed cell-size distribution (Fig. 3), and instead resulted in very narrow distributions that were considerably different from the expected skewed, right-tailed shape (Tables 2, 3). In agreement with the neo-cellular theory, the models supported the need for an organ-wide control of cell growth as a key mechanism to increase cell size variance, and pointed to a direct effect of ploidy on cell expansion potential.

Measurement of cell size distribution: a promising approach to understand the control of fruit growth

Our study was based on the analysis of cell-size distribution as a footprint of different control schemes. The NRMSE values of our results with respect to the pericarp fresh and dry mass data were always between 20% and 30% and this was independent of the model variant and the tomato genotype (Tables 2, 3), indicating a satisfactory agreement with the observed data. This highlights the

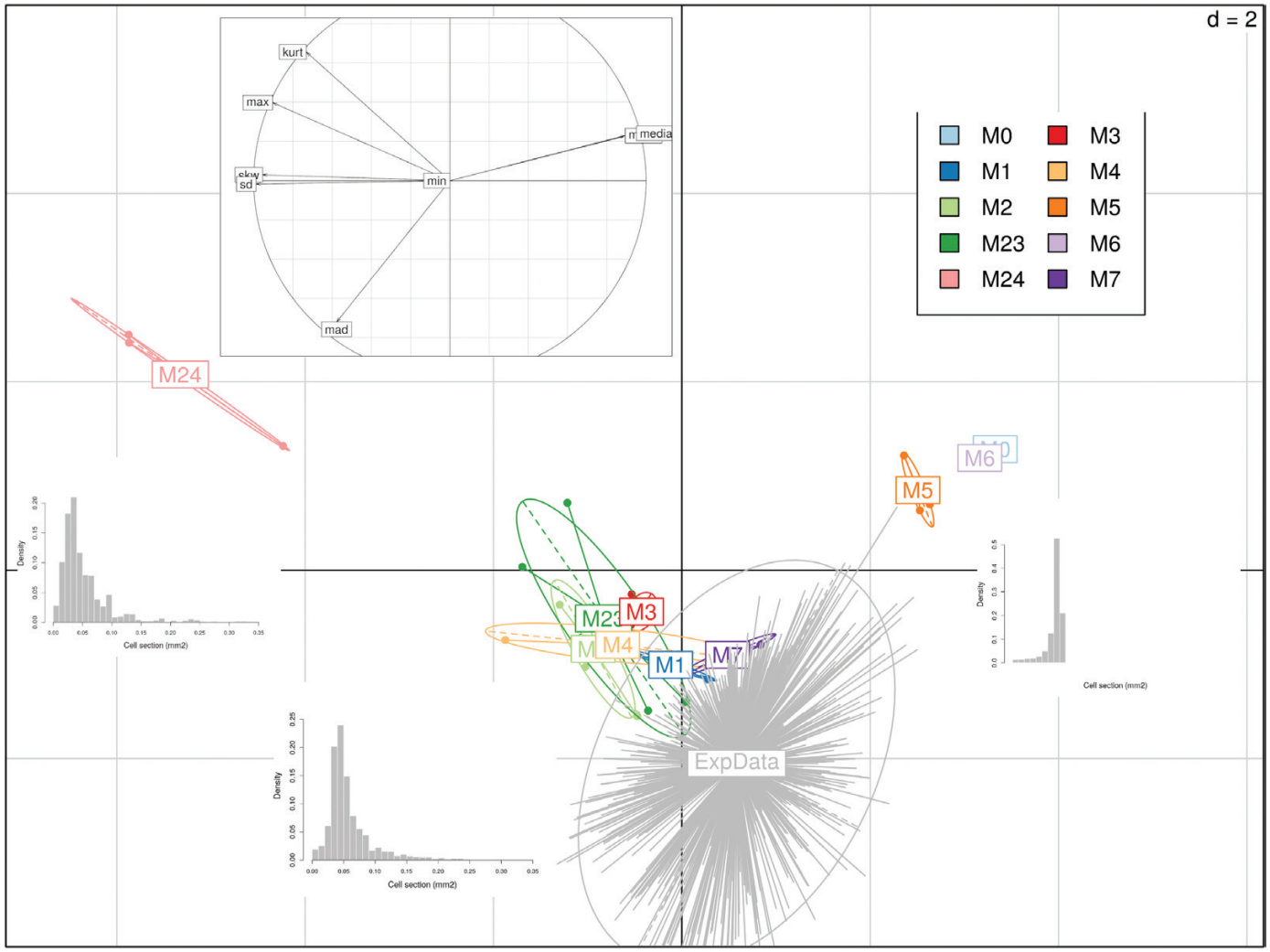

Fig. 6. Principal component analysis (PCA) of cell-size distributions obtained for the large-fruited tomato genotype Levovil using the model variants M0–M24 (Table 1). The main plot shows the projection of individual distributions on the PC1–PC2 plane (75% and 17% of variance explained, respectively); *d* is the grid unit. Bootstrap results for measured cell size data are also projected (ExpData) as supplementary observations. Typical cell-size distribution shapes are illustrated for the main subgroups. Correlations of the variables with the first two principal components are shown in the inset at the top.

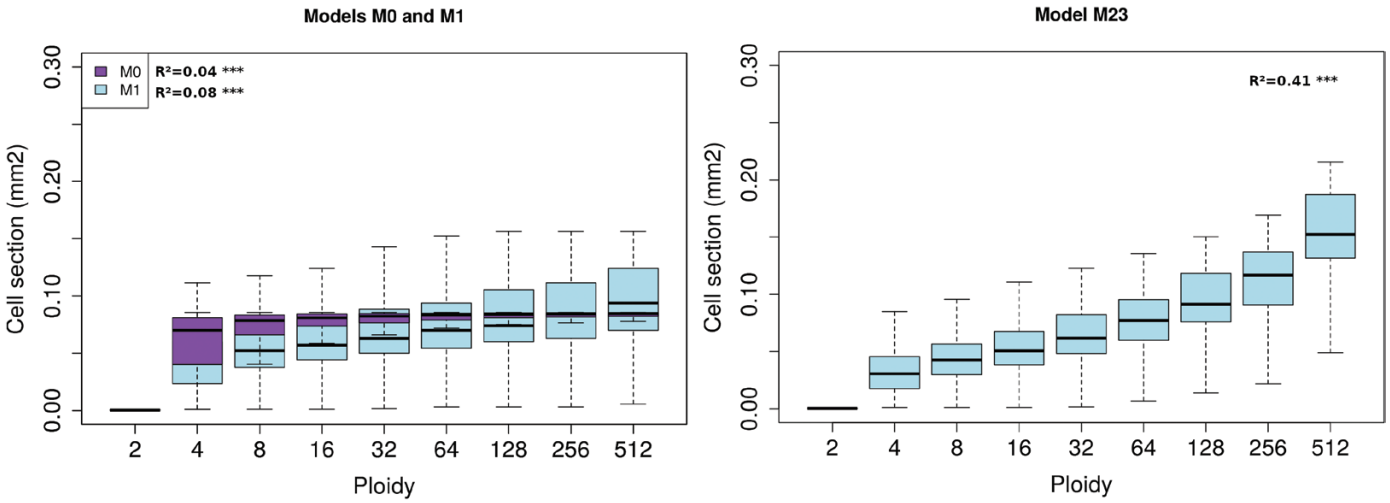

Fig. 7. Simulated relationships between ploidy and cell size at fruit maturity for the large-fruited tomato Levovil genotype. Left, models M0 and M1; and right, model M23 (Table 1). The adjusted R^2 values corresponding to a linear regression model are shown. (This figure is available in colour at *JXB* online.)

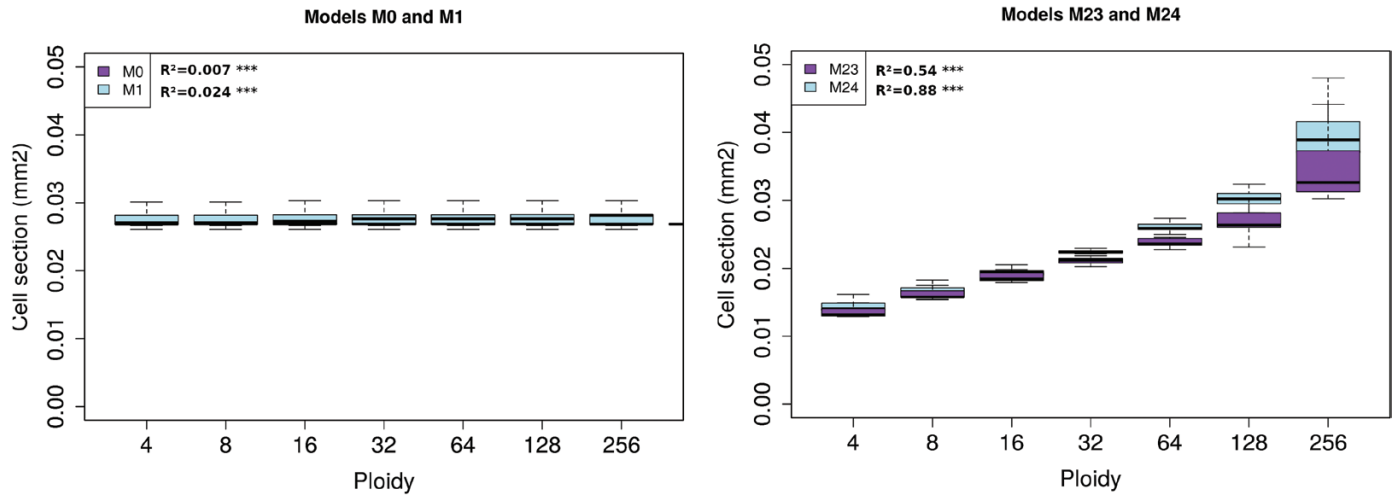

Fig. 8. Simulated relationships between ploidy and cell size at fruit maturity for the cherry tomato Cervil genotype. Left, models M0 and M1; and right, models M23 and M24 (Table 1). The adjusted R^2 values corresponding to a linear regression model are shown. (This figure is available in colour at *JXB* online.)

fact that the dynamics of fruit growth alone are not enough to discriminate between several biologically plausible models. In this sense, cell-size distribution represents a much more informative dataset as it uniquely results from the specific cell division and expansion patterns of the organ (Halter *et al.*, 2009).

The assessment of cell sizes in an organ is not an easy task, however, and the measurement technique that is chosen may have important consequences on the resulting cell-size distribution that is obtained (Legland *et al.*, 2012). Mechanical constraints acting on tissues as well as vascularization can significantly modify cell shape, resulting in elongated or multilobed cells (Ivakov and Persson, 2013). Thus, in situations where the orientation of 2D slices can potentially affect the resulting estimation of cell area, possible differences between *in vivo* tissues and dissociated cells should be systematically checked (McAtee *et al.*, 2009). The size of the dataset is also important with regards to correctly characterizing the expected shape of the distribution. Indeed, outliers can significantly affect the estimation of high-order moments, especially in long-tailed distributions such as those usually observed in plant organs. It is for these reasons that we decided to focus on a qualitative comparison of simulated and experimental cell size distribution rather than on a 'perfect fit'. Uncertainty in our dataset was accounted for via the estimation of confidence intervals for the experimental distribution moments.

In terms of future developments, the use of mutant or modified varieties (Musseau *et al.*, 2017) in combination with recent advancements in microscopy and tomography may permit the acquisition of more reliable datasets, thus opening the way to an in-depth investigation of cell-size distribution in relation to fruit tissues and hence to the underlying molecular processes (Mebatsion *et al.*, 2009; Wuyts *et al.*, 2010).

The relative importance of organ-wide and ploidy-dependent controls may be genotype-dependent

According to our models, organ-wide control was responsible for cell-to-cell variations but a ploidy-mediated effect on cell expansion was needed in order to obtain a significant correlation between size and ploidy (Figs 7, 8), as is observed in experimental data for fruit pericarps (Bourdon *et al.*, 2011). However, the relative importance of the two modes of control may be genotype-dependent.

For the large-fruited variety, Levovil, organ-wide control was the dominant mechanism (Fig. 6). This was probably due to its long division phase, which causes the appearance of new, expanding cells late in the development of the fruit, once closure of the plasmodesmata is already completed. Independently of the targeted process, the addition of a ploidy-dependent effect did not significantly modify the predicted cell-size distribution. The models supported the idea that cell ploidy may fix a maximum potential growth rate. Given the large fruit mass in the Levovil genotype, it is possible that such a potential may not have been fully reached in our experimental conditions, due to limited plant resources.

In the case of the cherry tomato variety, Cervil, the effect of a ploidy-dependent mechanism was more pronounced, especially when affecting cell carbon metabolism. Models combining both an organ- and a ploidy-dependent control performed better than the others (Fig. 5), although they failed to fully account for the experimental cell-size distribution. There may be a number of reasons for this discrepancy. First, due to a lack of data, the endoreduplication dynamics were calibrated according to the 2004 experiment whereas the division and the expansion modules were estimated using the 2007 data, where the cell-size distribution was available. Little is known about the possible dependence of endoreduplication on environmental variables (Engelen-Eigles *et al.*, 2000; Setter and Flannigan, 2001; Cookson *et al.*, 2006). In tomato fruit, changes in ploidy levels are mainly linked to changes in the duration of the mitotic phase (Bertin, 2005) but a direct effect of environmental fluctuations on endoreduplication-related parameters cannot be excluded. This may be particularly true for the cherry tomato genotype, for which the dynamics of cell division differed significantly between the two years (Supplementary Protocol S3). It could therefore be expected that the progression of the endocycle

may also have been different, with possible consequences on the shape of the resulting cell-size distribution. Preliminary simulations showed that an acceleration of the endocycle or an increase of the proportion of cells that entered a new round of endoreduplication could spread the resulting distribution towards large cell sizes, increasing the overall variance in models that included a ploidy-dependent effect.

In addition to mechanisms related to the cell cycle, environment and cultural practices can also affect the resource availability at the cell scale. In many fruit species including tomato, a negative correlation between mean cell size and cell number has been observed, suggesting the existence of competition for resources (Prudent *et al.*, 2014). This kind of mechanism may widen the range of attainable cell sizes, and increase size variations between early- and late-initiated cells. The importance of such an effect may vary with genotype and environmental conditions (Bertin, 2005; Quilot and Génard, 2008).

Stochasticity in cellular processes may be important for explaining cell-size variance in fruit

Our model is an example of a population model: the fruit is described as a collection of cell groups, each having specific characteristics in terms of number, mass, age, and ploidy level that dynamically evolve over time. Although asynchrony in the emergence of cell groups allowed us to capture a reasonable part of cell-to-cell heterogeneity (Tables 2, 3, Dispersion), the intrinsic stochasticity of cellular processes (Robinson *et al.*, 2011; De Smet and Beeckman, 2011; Meyer and Roeder, 2014) was not accounted for. Variations in the threshold size for division (often associated with a change in the cell cycle duration) as well as asymmetric cell divisions are considered as important determinants of the final cell size (Dupuy *et al.*, 2010; Roeder *et al.*, 2010; Stukalin *et al.*, 2013; Osella *et al.*, 2014), and they may contribute to significantly spreading the size distribution of both the proliferating and expanding cell groups from early stages. Moreover, the degree of additional dispersion introduced by cell expansion is likely to depend on the specificity of the underlying mechanisms, with possible interactions with ploidy-dependent and organ-wide controls.

In terms of future developments, the addition of stochastic effects could help to fill the missing variance for both cherry and large-fruited genotypes. To achieve this, a novel modelling scheme is needed in which the mean cell size of a group is replaced by a distribution of cell sizes, the parameters of which can evolve with time under the effect of cell expansion processes.

Correlation between size and ploidy: a clue for a direct influence of endoreduplication on cell expansion in tomato fruit?

Our results showed that asynchrony in cell division and endoreduplication events prevented the emergence of a correlation between size and ploidy based only on time course. According to our present model, a direct effect of nuclear ploidy on the attainable cell growth rate is needed in order to obtain the observed correlation in tomato fruit. This is in line with data in the literature that points to the ploidy level setting the maximum cell growth rate that can be attained, with the actual rate depending on internal (hormones) and external (environmental) factors (Breuer *et al.*, 2010; Chevalier *et al.*, 2011; De Veylder *et al.*, 2011). Of course, this may be less striking in systems where the progression of endocycles is more sequential. An example may be the sepals of Arabidopsis, where data are consistent with a model in which expanding cells undergo a new round of endoreduplication at each time-step (Roeder *et al.*, 2010). In this system, variability among cell size arises from asymmetry in cell division and variations in the exit time from mitotic cycle, whilst no differences in the growth rate are observed among cells with different ploidy levels (Tauriello *et al.*, 2015; Robinson *et al.*, 2018).

Overall, these results confirm that the relationship between endoreduplication and expansion may not be universal but can differ depending on the organ being considered. Moreover, attention should also be payed to cell identity. Thus, quantitative differences in the strength of the ploidy-dependent effect have been demonstrated between pavement and mesophyll cells in Arabidopsis leaves (Katagiri *et al.*, 2016; Kawade and Tsukaya, 2017), whilst cell layer-specific developmental patterns have been observed in tomato fruit (Renaudin *et al.* 2017). In the model that we have developed, the spatial distribution of expanding-endoreduplicating cells is not accounted for. In terms of future developments, a model that includes distinct cell-layer populations with specific expansion programs may help to refine the relationship between ploidy and size.

Ultimately, improvements in the ability of computation models to integrate the multiple facets of organ development in a mechanistic way can help to evaluate and quantify the contribution of the different processes to the control of cell growth.

Supplementary data

Supplementary data are available at *JXB* online.

Protocol S1. Cell distribution fit.

Protocol S2. Model equations and implementation.

Protocol S3. Model calibration and estimated parameter values.

Protocol S4. Correlation between ploidy and size.

Acknowledgements

The authors warmly thank B. Brunel for help with cell measurements. The authors are grateful to Inria Sophia Antipolis – Méditerranée 'NEF' computation cluster for providing resources and support. This work was partially funded by the Agence Nationale de la Recherche, Project 'Frimouss' (grant no. ANR–15–CE20–0009) and by the Agropolis Foundation under the reference ID 1403-032 through the « Investissements d'avenir » programme (Labex Agro:ANR-10-LABX-0001-01).

References

Asl LK, Dhondt S, Boudolf V, Beemster GT, Beeckman T, Inzé D, Govaerts W, De Veylder L. 2011. Model-based analysis of Arabidopsis

leaf epidermal cells reveals distinct division and expansion patterns for pavement and guard cells. Plant Physiology **156**, 2172–2183.

Baldazzi V, Bertin N, Genard M, Génard M. 2012. A model of fruit growth integrating cell division and expansion processes. Acta Horticulturae **957**, 191–196.

Baldazzi V, Génard M, Bertin N. 2017. Cell division, endoreduplication and expansion processes: setting the cell and organ control into an integrated model of tomato fruit development. Acta Horticulturae **1182**, 257–264

Baldazzi V, Pinet A, Vercambre G, Bénard C, Biais B, Génard M. 2013. *In-silico* analysis of water and carbon relations under stress conditions. A multi-scale perspective centered on fruit. Frontiers in Plant Science **4**, 495.

Barow M. 2006. Endopolyploidy in seed plants. BioEssays **28**, 271–281.

Beemster GT, Fiorani F, Inzé D. 2003. Cell cycle: the key to plant growth control? Trends in Plant Science **8**, 154–158.

Bertin N. 2005. Analysis of the tomato fruit growth response to temperature and plant fruit load in relation to cell division, cell expansion and DNA endoreduplication. Annals of Botany **95**, 439–447.

Bertin N, Genard M, Fishman S. 2003. A model for an early stage of tomato fruit development: cell multiplication and cessation of the cell proliferative activity. Annals of Botany **92**, 65–72.

Bertin N, Lecomte A, Brunel B, Fishman S, Génard M. 2007. A model describing cell polyploidization in tissues of growing fruit as related to cessation of cell proliferation. Journal of Experimental Botany **58**, 1903–1913.

Boudon F, Chopard J, Ali O, Gilles B, Hamant O, Boudaoud A, Traas J, Godin C. 2015. A computational framework for 3D mechanical modeling of plant morphogenesis with cellular resolution. PLoS Computational Biology **11**, e1003950.

Bourdon M, Coriton O, Pirrello J, Cheniclet C, Brown SC, Poujol C, Chevalier C, Renaudin JP, Frangne N. 2011. *In planta* quantification of endoreduplication using fluorescent *in situ* hybridization (FISH). The Plant Journal **66**, 1089–1099.

Breuer C, Ishida T, Sugimoto K. 2010. Developmental control of endocycles and cell growth in plants. Current Opinion in Plant Biology **13**, 654–660.

Bünger-Kibler S, Bangerth F. 1982. Relationship between cell number, cell size and fruit size of seeded fruits of tomato (*Lycopersicon esculentum* Mill.), and those induced parthenocarpically by the application of plant growth regulators. Plant Growth Regulation **1**, 143–154.

Carrari F, Baxter C, Usadel B, *et al*. 2006. Integrated analysis of metabolite and transcript levels reveals the metabolic shifts that underlie tomato fruit development and highlight regulatory aspects of metabolic network behavior. Plant Physiology **142**, 1380–1396.

Cheniclet C, Rong WY, Causse M, Frangne N, Bolling L, Carde JP, Renaudin JP. 2005. Cell expansion and endoreduplication show a large genetic variability in pericarp and contribute strongly to tomato fruit growth. Plant Physiology **139**, 1984–1994.

Chevalier C, Bourdon M, Pirrello J, Cheniclet C, Gévaudant F, Frangne N. 2014. Endoreduplication and fruit growth in tomato: evidence in favour of the karyoplasmic ratio theory. Journal of Experimental Botany **65**, 2731–2746.

Chevalier C, Nafati M, Mathieu-Rivet E, Bourdon M, Frangne N, Cheniclet C, Renaudin JP, Gévaudant F, Hernould M. 2011. Elucidating the functional role of endoreduplication in tomato fruit development. Annals of Botany **107**, 1159–1169.

Colombié S, Nazaret C, Bénard C, *et al*. 2014. Modelling central metabolic fluxes by constraint-based optimization reveals metabolic reprogramming of developing *Solanum lycopersicum* (tomato) fruit. The Plant Journal **81**, 24–39.

Constantinescu D, Memmah MM, Vercambre G, Génard M, Baldazzi V, Causse M, Albert E, Brunel B, Valsesia P, Bertin N. 2016. Model-assisted estimation of the genetic variability in physiological parameters related to tomato fruit growth under contrasted water conditions. Frontiers in Plant Science **7**, 1841.

Cookson SJ, Radziejwoski A, Granier C. 2006. Cell and leaf size plasticity in Arabidopsis: what is the role of endoreduplication? Plant, Cell & Environment **29**, 1273–1283.

Cosgrove DJ. 2016. Plant cell wall extensibility: connecting plant cell growth with cell wall structure, mechanics, and the action of wall-modifying enzymes. Journal of Experimental Botany **67**, 463–476.

Crawford KM, Zambryski PC. 2001. Non-targeted and targeted protein movement through plasmodesmata in leaves in different developmental and physiological states. Plant Physiology **125**, 1802–1812.

De Smet I, Beeckman T. 2011. Asymmetric cell division in land plants and algae: the driving force for differentiation. Nature Reviews Molecular Cell Biology **12**, 177–188.

De Veylder L, Larkin JC, Schnittger A. 2011. Molecular control and function of endoreplication in development and physiology. Trends in Plant Science **16**, 624–634.

Dupuy L, Mackenzie J, Haseloff J. 2010. Coordination of plant cell division and expansion in a simple morphogenetic system. Proceedings of the National Academy of Sciences, USA **107**, 2711–2716.

Edgar BA, Zielke N, Gutierrez C. 2014. Endocycles: a recurrent evolutionary innovation for post-mitotic cell growth. Nature Reviews Molecular Cell Biology **15**, 197–210.

Engelen-Eigles G, Jones RJ, Phillips RL. 2000. DNA endoreduplication in maize endosperm cells: the effect of exposure to short-term high temperature. Plant, Cell and Environment **23**, 657–663.

Fanwoua J, de Visser P, Heuvelink E, Yin X, Struik PC, Marcelis LFM. 2013. A dynamic model of tomato fruit growth integrating cell division, cell growth and endoreduplication. Functional Plant Biology **40**, 1098.

Ferjani A, Horiguchi G, Yano S, Tsukaya H. 2007. Analysis of leaf development in *fugu* mutants of Arabidopsis reveals three compensation modes that modulate cell expansion in determinate organs. Plant Physiology **144**, 988–999.

Fishman S, Génard M. 1998. A biophysical model of fruit growth: simulation of seasonal and diurnal dynamics of mass. Plant, Cell and Environment **21**, 739–752.

Fleming AJ. 2006. The integration of cell proliferation and growth in leaf morphogenesis. Journal of Plant Research **119**, 31–36.

Halter M, Elliott JT, Hubbard JB, Tona A, Plant AL. 2009. Cell volume distributions reveal cell growth rates and division times. Journal of Theoretical Biology **257**, 124–130.

Han X, Kumar D, Chen H, Wu S, Kim JY. 2014. Transcription factor-mediated cell-to-cell signalling in plants. Journal of Experimental Botany **65**, 1737–1749.

Horiguchi G, Tsukaya H. 2011. Organ size regulation in plants: insights from compensation. Frontiers in Plant Science **2**, 24.

Ivakov A, Persson S. 2013. Plant cell shape: modulators and measurements. Frontiers in Plant Science **4**, 439.

Jégu T, Latrasse D, Delarue M, *et al*. 2013. Multiple functions of Kip-related protein5 connect endoreduplication and cell elongation. Plant Physiology **161**, 1694–1705.

John PCL, Qi R. 2008. Cell division and endoreduplication: doubtful engines of vegetative growth. Trends in Plant Science **13**, 121–127.

Katagiri Y, Hasegawa J, Fujikura U, Hoshino R, Matsunaga S, Tsukaya H. 2016. The coordination of ploidy and cell size differs between cell layers in leaves. Development **143**, 1120–1125.

Kawade K, Horiguchi G, Tsukaya H. 2010. Non-cell-autonomously coordinated organ size regulation in leaf development. Development **137**, 4221–4227.

Kawade K, Tsukaya H. 2017. Probing the stochastic property of endoreduplication in cell size determination of Arabidopsis thaliana leaf epidermal tissue. PLoS ONE **12**, e0185050.

Kuchen EE, Fox S, de Reuille PB, *et al*. 2012. Generation of leaf shape through early patterns of growth and tissue polarity. Science **335**, 1092–1096.

Legland D, Devaux MF, Bouchet B, Guillon F, Lahaye M. 2012. Cartography of cell morphology in tomato pericarp at the fruit scale. Journal of Microscopy **247**, 78–93.

Liu HF, Génard M, Guichard S, Bertin N. 2007. Model-assisted analysis of tomato fruit growth in relation to carbon and water fluxes. Journal of Experimental Botany **58**, 3567–3580.

Lockhart JA. 1965. An analysis of irreversible plant cell elongation. Journal of Theoretical Biology **8**, 264–275.

Löfke C, Dünser K, Scheuring D, *et al*. 2015. Auxin regulates SNARE-dependent vacuolar morphology restricting cell size. eLIFE **4**, 119–122.

Lucas M, Kenobi K, von Wangenheim D, *et al*. 2013. Lateral root morphogenesis is dependent on the mechanical properties of the overlaying

tissues. Proceedings of the National Academy of Sciences, USA **110**, 5229–5234.

McAtee PA, Hallett IC, Johnston JW, Schaffer RJ. 2009. A rapid method of fruit cell isolation for cell size and shape measurements. Plant Methods **5**, 5.

Mebatsion HK, Verboven P, Melese Endalew A, Billen J, Ho QT, Nicolaï BM. 2009. A novel method for 3-D microstructure modeling of pome fruit tissue using synchrotron radiation tomography images. Journal of Food Engineering **93**, 141–148.

Meyer HM, Roeder AHK. 2014. Stochasticity in plant cellular growth and patterning. Frontiers in Plant Science **5**, 420.

Musseau C, Just D, Jorly J, Gvaudant F, Moing A, Chevalier C, Lemaire-Chamley M, Rothan C, Fernandez L. 2017. Identification of two new mechanisms that regulate fruit growth by cell expansion in tomato. Frontiers in Plant Science **8**, 988.

Norman JM. Van, Breakfield NW, Benfey PN, Carolina N, Van Norman JM, Breakfield NW, Benfey PN. 2011. Intercellular communication during plant development. The Plant Cell **23**, 855–864.

Okello RCO, Heuvelink E, de Visser P, Struik PC, Marcelis LFM. 2015. What drives fruit growth? Functional Plant Biology **42**, 817.

Osella M, Nugent E, Cosentino Lagomarsino M. 2014. Concerted control of *Escherichia coli* cell division. Proceedings of the National Academy of Sciences, USA **111**, 4–8.

Pirrello J, Deluche C, Frangne N, *et al*. 2018. Transcriptome profiling of sorted endoreduplicated nuclei from tomato fruits: how the global shift in expression ascribed to DNA ploidy influences RNA-Seq data normalization and interpretation. The Plant Journal **93**, 387–398.

Proseus TE, Boyer JS. 2006. Identifying cytoplasmic input to the cell wall of growing *Chara corallina*. Journal of Experimental Botany **57**, 3231–3242.

Proseus TE, Ortega JK, Boyer JS. 1999. Separating growth from elastic deformation during cell enlargement. Plant Physiology **119**, 775–784.

Prudent M, Dai ZW, Génard M, Bertin N, Causse M, Vivin P. 2014. Resource competition modulates the seed number–fruit size relationship in a genotype-dependent manner: a modeling approach in grape and tomato. Ecological Modelling **290**, 54–64

Quilot B, Génard M. 2008. Is competition between mesocarp cells of peach fruits affected by the percentage of wild species genome? Journal of Plant Research **121**, 55–63.

Renaudin JP, Deluche C, Cheniclet C, Chevalier C, Frangne N. 2017. Cell layer-specific patterns of cell division and cell expansion during fruit set and fruit growth in tomato pericarp. Journal of Experimental Botany **68**, 1613–1623.

Robinson DO, Coate JE, Singh A, Hong L, Bush M, Doyle JJ, Roeder AHK, Jeff J. 2018. Ploidy and size at multiple scales in the Arabidopsis sepal. The Plant Cell **30**, 2308–2329.

Robinson S, Barbier de Reuille P, Chan J, Bergmann D, Prusinkiewicz P, Coen E. 2011. Generation of spatial patterns through cell polarity switching. Science **333**, 1436–1440.

Roeder AHK, Chickarmane V, Cunha A, Obara B, Manjunath BS, Meyerowitz EM. 2010. Variability in the control of cell division underlies sepal epidermal patterning in *Arabidopsis thaliana*. PLoS Biology **8**, e1000367.

Sablowski R, Carnier Dornelas M. 2014. Interplay between cell growth and cell cycle in plants. Journal of Experimental Botany **65**, 2703–2714.

Schoenfelder KP, Fox DT. 2015. The expanding implications of polyploidy. The Journal of Cell Biology **209**, 485–91.

Serrano-Mislata A, Schiessl K, Sablowski R. 2015. Active control of cell size generates spatial detail during plant organogenesis. Current Biology **25**, 2991–2996.

Setter TL, Flannigan BA. 2001. Water deficit inhibits cell division and expression of transcripts involved in cell proliferation and endoreduplication in maize endosperm. Journal of Experimental Botany **52**, 1401–1408.

Stukalin EB, Aifuwa I, Kim JS, Wirtz D, Sun SX. 2013. Age-dependent stochastic models for understanding population fluctuations in continuously cultured cells. Journal of the Royal Society Interface **10**, 20130325.

Sugimoto-Shirasu K, Roberts K. 2003. "Big it up": endoreduplication and cell-size control in plants. Current Opinion in Plant Biology **6**, 544–553.

Tauriello G, Meyer HM, Smith RS, Koumoutsakos P, Roeder AH. 2015. Variability and constancy in cellular growth of Arabidopsis sepals. Plant Physiology **169**, 2342–2358.

Thompson DS, Davies WJ, Ho LC. 1998. Regulation of tomato fruit growth by epidermal cell wall enzymes. Plant, Cell and Environment **21**, 589–599.

Tsukaya H. 2003. Organ shape and size: a lesson from studies of leaf morphogenesis. Current Opinion in Plant Biology **6**, 57–62.

von Wangenheim D, Fangerau J, Schmitz A, Smith RS, Leitte H, Stelzer EH, Maizel A. 2016. Rules and self-organizing properties of post-embryonic plant organ cell division patterns. Current Biology **26**, 439–449.

Wuyts N, Palauqui JC, Conejero G, Verdeil JL, Granier C, Massonnet C. 2010. High-contrast three-dimensional imaging of the Arabidopsis leaf enables the analysis of cell dimensions in the epidermis and mesophyll. Plant Methods **6**, 17.

Zambryski PC. 2004. Cell-to-cell transport of proteins and fluorescent tracers via plasmodesmata during plant development. Journal of Cell Biology **164**, 165–168.